



Fuel Injector Design Optimization for an Annular Scramjet Geometry

Christopher J. Steffen, Jr.
Glenn Research Center, Cleveland, Ohio

The NASA STI Program Office . . . in Profile

Since its founding, NASA has been dedicated to the advancement of aeronautics and space science. The NASA Scientific and Technical Information (STI) Program Office plays a key part in helping NASA maintain this important role.

The NASA STI Program Office is operated by Langley Research Center, the Lead Center for NASA's scientific and technical information. The NASA STI Program Office provides access to the NASA STI Database, the largest collection of aeronautical and space science STI in the world. The Program Office is also NASA's institutional mechanism for disseminating the results of its research and development activities. These results are published by NASA in the NASA STI Report Series, which includes the following report types:

- TECHNICAL PUBLICATION. Reports of completed research or a major significant phase of research that present the results of NASA programs and include extensive data or theoretical analysis. Includes compilations of significant scientific and technical data and information deemed to be of continuing reference value. NASA's counterpart of peer-reviewed formal professional papers but has less stringent limitations on manuscript length and extent of graphic presentations.

• TECHNICAL MEMORANDUM. Scientific and technical findings that are preliminary or of specialized interest, e.g., quick release reports, working papers, and bibliographies that contain minimal annotation. Does not contain extensive analysis.

- CONTRACTOR REPORT. Scientific and technical findings by NASA-sponsored contractors and grantees.

• CONFERENCE PUBLICATION. Collected papers from scientific and technical conferences, symposia, seminars, or other meetings sponsored or cosponsored by NASA.

- SPECIAL PUBLICATION. Scientific, technical, or historical information from NASA programs, projects, and missions, often concerned with subjects having substantial public interest.
- TECHNICAL TRANSLATION. English-language translations of foreign scientific and technical material pertinent to NASA's mission.

Specialized services that complement the STI Program Office's diverse offerings include creating custom thesauri, building customized databases, organizing and publishing research results . . . even providing videos.

For more information about the NASA STI Program Office, see the following:

- Access the NASA STI Program Home Page at <http://www.sti.nasa.gov>
- E-mail your question via the Internet to help@sti.nasa.gov
- Fax your question to the NASA Access Help Desk at 301-621-0134
- Telephone the NASA Access Help Desk at 301-621-0390
- Write to:
NASA Access Help Desk
NASA Center for AeroSpace Information
7121 Standard Drive
Hanover, MD 21076



Fuel Injector Design Optimization for an Annular Scramjet Geometry

Christopher J. Steffen, Jr.
Glenn Research Center, Cleveland, Ohio

Prepared for the
41st Aerospace Sciences Meeting and Exhibit
sponsored by the American Institute of Aeronautics and Astronautics
Reno, Nevada, January 6–9, 2003

National Aeronautics and
Space Administration

Glenn Research Center

January 2003

This report contains preliminary findings, subject to revision as analysis proceeds.

Trade names or manufacturers' names are used in this report for identification only. This usage does not constitute an official endorsement, either expressed or implied, by the National Aeronautics and Space Administration.

The Propulsion and Power Program at
NASA Glenn Research Center sponsored this work.

Available from

NASA Center for Aerospace Information
7121 Standard Drive
Hanover, MD 21076

National Technical Information Service
5285 Port Royal Road
Springfield, VA 22100

Available electronically at <http://gltrs.grc.nasa.gov>

Fuel Injector Design Optimization for an Annular Scramjet Geometry

Christopher J. Steffen, Jr.*

National Aeronautics and Space Administration
Glenn Research Center
Cleveland, Ohio 44135
C.J.steffen@grc.nasa.gov

Abstract

A four-parameter, three-level, central composite experiment design has been used to optimize the configuration of an annular scramjet injector geometry using computational fluid dynamics. The computational fluid dynamic solutions played the role of computer experiments, and response surface methodology was used to capture the simulation results for mixing efficiency and total pressure recovery within the scramjet flowpath. An optimization procedure, based upon the response surface results of mixing efficiency, was used to compare the optimal design configuration against the target efficiency value of 92.5%. The results of three different optimization procedures are presented and all point to the need to look outside the current design space for different injector geometries that can meet or exceed the stated mixing efficiency target.

Introduction

NASA is presently studying several advanced propulsion systems that promise to provide affordable access to space. One concept, the reusable SSTO “GTX,” is a rocket-based-combined cycle (RBCC) propulsion system. A three-view schematic is shown in Figure 1. An axisymmetric engine design has been created with an emphasis placed upon structural and analytical simplicity. The flowpath is defined by a fixed cowl and a translating centerbody which allows for the required variable geometry (see Figure 1).

The operational scenario for GTX consists of four modes of propulsion. In the first mode, valid from liftoff to about Mach 2.5, the engine operates in a so-called independent ramjet stream (IRS) cycle, where rocket thrust is initially used for primary power and as an ignition source for hydrogen fuel injected directly into the inlet air. Ignition and combustion of this fuel source results in the formation of a thermal throat in the nozzle, and a ramjet mode of operation for the secondary stream. As the Mach number increases, the percentage of thrust due to the ramjet alone increases, and around Mach 2.5, the rocket motor is shut off and the engine shifts to a pure ramjet mode of operation (second mode). Around Mach 6, it becomes more practical to burn at supersonic speeds, and aided by centerbody translation, the engine shifts to a scramjet mode (third mode). The rocket is re-ignited around Mach 11 (fourth mode), the centerbody is translated to shut the inlet flow completely off, and the engine shifts to a rocket-only propulsion mode for the remainder of the ascent. Further details on the operation of this propulsion cycle are available in reference.¹

The single flowpath concept presents a design challenge for the fuel injectors within this air-breathing combustor. Parametric CFD analysis can be used in a cost-effective manner to address this problem. Initial simulations can be done to screen the significant design parameters which deserve further study. Next, a detailed parametric analysis can be executed such that a polynomial response model can be developed to capture the relevant performance parameters. Design optimization, based upon the

* Senior Member, AIAA

response surface modeling results, can point towards the optimal injector configuration within the design space. This three-step process has been carried out for the GTx combustor geometry, during mode three operation.

Summary of Screening Design Results

An initial screening design was conducted to investigate the importance of five design parameters governing the fuel injector²

- (x_1) Injector angle (α_{inj}) relative to wall
- (x_2) Injector location (X_{inj}), relative to engine station #3 (see Figure 2)
- (x_3) Flight mach number (M_o)
- (x_4) Fuel/Air ratio (ϕ_{inj})
- (x_5) Fuel split between axial and transverse injectors (a mixture variable)

Results of this first phase of analysis clearly indicated that total fuel/air ratio should be maximized and axial fuel injector massflow should be minimized for the best mixing efficiency of injector geometry at all Mach numbers. Other significant effects were observed, but the sparse nature of the screening design obfuscated the results. More to the point, extensive confirmation testing revealed that a probable three-way interaction was lurking in the dataset, yet unresolved with the screening design. The sparse nature of the screening design can be appreciated after examining the schematic representation of a half-fractional, central composite design shown in Figure 4.

Objective for RSM Design

A more focused, second phase of this analysis was undertaken to develop accurate response models for both the mixing efficiency and total pressure recovery. This second phase concentrated upon the first four parameters discussed above, and fixed the fuel split parameter at one condition (25% step injector—75% transverse injector). The second phase was comprised of a central composite experiment design in four parameters, shown in Figure 5. This design was capable of resolving the linear, quadratic, two-way and three-way interactions that were anticipated. This polynomial regression model, in turn, has been used as a surrogate for the costly CFD analysis during the process of design optimization. The optimization process sought answers to the following two questions: 1) Which injector geometry yields the best integrated performance of mixing efficiency across the scram trajectory? and 2) Can we meet the design target efficiency of 92.5% across the scram trajectory with the current injector design philosophy?

Numerical Methods

The Navier-Stokes solver used for these solutions was the GASPv4 code. GASP is a 3D, finite volume, structured-mesh RANS solver that has been used to analyze many high-speed propulsion flows, including scramjet combustors, in steady state or time-dependent fashion. A detailed discussion of the numerical methods have been presented elsewhere.²

The scramjet flowfield was assumed to be mixing limited, and thus the simulations have been executed with frozen chemistry. The GTx combustor geometry was designed as a 220° annular section, with planar endwalls. The scramjet CFD simulations neglect the endwall effect and assumed a full 360° engine geometry. This simplification enabled the computational domain to be limited by the fuel injector symmetry requirement. The circumferential distribution of injectors was fixed at three-degrees for the axial injectors and six-degrees for the transverse injectors. The percentage of fuel entering the combustor through the axial injectors was fixed at 25%. The combustor entrance conditions were specified from decoupled axisymmetric inlet simulations, according to the freestream conditions along a prescribed trajectory.³ The injectors have been specified as choked, sonic conditions for all cases. The gaseous hydrogen fuel was injected with a static temperature that varied with freestream Mach number. The fuel temperatures were specified as (1500, 2000, and 2500 °R) at Mach (6.5, 9.25, and 12) respectively.

All results have been converged so that massflux was constant to within $\pm 1\%$. The mesh dependence of these results has been taken as approximately $\pm 5\%$ based upon three different simulations with a coarse/fine grid sequence of (280k/2.24M) cells.⁴ An examination of the run matrix indicates that the mixing efficiency results vary by as much as 64% across this design space. The results presented below have included an uncertainty associated with the response surface model predictions. The 95% confidence interval was seen to be slightly larger than the simulation errors discussed above. Note that this confidence interval is strictly valid for a normally distributed error, which is not the case with “computer experiments” of this type. Nevertheless, one can treat this bound as a reasonably conservative estimate of error since the dominant CFD errors (mesh dependence and iterative convergence) are of lesser magnitude. The field of experiment design for “computer experiments” is an active research area, and the interested reader is referred elsewhere for further reading.²

Two response variables have been modeled with RSM: the mixing efficiency of the hydrogen fuel and the total pressure recovery within the combustor. The mixing efficiency was defined as the percentage of oxygen that would be present in product water, if the flow was allowed to reach chemical equilibrium without further mixing. The species oxygen was chosen instead of hydrogen because all of the conditions considered herein are stoichiometric or fuel rich. Total pressure recovery was simply defined as the stream-thrust-averaged total pressure at the combustor exit plane, relative to the combustor entrance plane.

Prior analysis has defined the combustor exit plane as the physical engine location called station #3 (see Figure 3). However, one-dimensional cycle analysis reveals that the combustion process must be completed at a specific area ratio which is inversely proportional to the flight Mach number (see Figure 6).[†] The reason for this is a fixed area profile throughout the mode three operation. To keep the Rayleigh losses in check during high Mach number flight, the combustion process must be completed at the lowest practical Mach number.⁵ This requirement can be expressed in terms of the combustor flowpath area ratio. This leads directly to a progressively shorter combustor length to achieve the target mixing efficiency. The area profile of the GTX flowpath through the scram combustor is given in Figure 7. It is readily apparent that the Mach 12 flight condition has considerably less combustor length than the Mach 6 condition, to achieve adequate fuel mixing. This occurs despite a higher Mach number inflow condition. The results that follow have been analyzed at the combustor exit locations given by Figure 6 and Figure 7.

Response Surface Results

A statistical analysis of the response data presented in Table 2 was performed using the software Design Expert™. The response surface model equations for the mixing efficiency and total pressure recovery are presented in the appendix, along with the standard error of prediction estimates. Thus far, a single confirmation case has been examined, and included in the data of Table 2 (as case #26). The observed value of mixing efficiency was (60.2%), while the RSM prediction was (63.8% with 95% confidence interval of [55.0%, 71.8%]). The observed value of total pressure recovery was (33.28%), while the RSM prediction was (33.54% with 95% confidence interval of [32.24%, 34.83%]).

The major conclusions of the previous work^{2,4} are consistent with the new statistical analysis. The primary difference is that the surrogate models presented in the appendix have captured a three-way interaction that was previously unaccounted for. This results in a much more appropriate polynomial for conducting the design optimization.

Two of the strongest effects present on the data can be seen[‡] in Figure 8. On average, increasing fuel equivalence ratio has an expected positive effect upon the mixing efficiency of a given geometry.

[†]Note that all flowpath area values have been rationalized by the captured streamtube area (A_{cap}).

[‡]Note that the 3D carpet plot is the response surface, the black dots correspond to data of Table 2, and vertical black bars are the standard-error-of-prediction bounds at 95% confidence. The experiment number from Table 2 has been included for reference purposes.

Likewise, flight Mach number was inversely proportional to mixing efficiency. These effects are well known for the scramjet combustor. Figure 9 shows the total pressure recovery over the same region.

The statistical analysis, combined with three-dimensional flow visualization, has brought to light an aspect of this engineering problem that would likely have been missed by conventional methods. The injector geometry (angle and location) and flight Mach number are involved in a three-way interaction. First, consider the interactive nature of the two geometric features, injector angle and location, at Mach 6.5 (see Figure 10). The interactive effect appears as a twist in the surface. Notice how the effect of injector angle upon mixing efficiency depended upon whether the injector was placed in the forward region (-115 in.) or the aft region (-90 in.). The results reveal that reducing the injection angle will improve the mixing in the forward region of the combustor, yet will have the opposite effect if located in the aft region. An explanation for this curious effect lies in the flow visualization taken from three-dimensional simulation results.

Consider the effect of different injector geometries at the ($M_o = 6.5, \phi_{inj} = 1.4$) condition. Figure 11 (Case #1) shows multiple cross-sections of the combustor flowfield between engine stations two and three. The injector geometry was low-angled ($\alpha_{inj} = 15^\circ$) and forward-located ($X_{inj} = -115$ in.). Contours of local equivalence ratio were used to indicate how well the oxygen has mixed with hydrogen fuel. Regions that appear as white or light gray are pockets of unmixed oxygen. Likewise, regions of black or dark gray are regions of high fuel concentration. Figure 11 clearly presents a well-mixed flow with good fuel penetration to the centerline of the annular flowpath. Figure 12 (Case #13) shows a similar figure with nearly the same configuration. The only difference from Case #1 was the injection angle ($\alpha_{inj} = 75^\circ$). One would expect even better fuel penetration for Case #13, and indeed this appears to be the case. However, the oxygen-rich flow appears to have been bifurcated into the two un-mixed regions that appear in the figure. Consequently, the mixing efficiency was lower than Case #1. To summarize, large injection angles are not necessary for the required fuel-jet penetration in the forward region of the combustor for the Mach 6.5, ($\phi_{inj} = 1.4$) condition.

Now consider the aft region of the combustor ($X_{inj} = -90$ in.). The gap between combustor walls is considerably larger in the aft region and the flow is substantially faster due to this area expansion. Figure 13 (Case #15) shows the results from the aft-located, low-angled injector at ($M_o = 6.5, \phi_{inj} = 1.4$). Now one can see that the hydrogen fuel never reaches the flowpath centerline. Instead, an oxygen-rich core flow has remained, and affects the overall mixing efficiency. Figure 14 (Case #4) corresponds to the aft-located, high-angled injector. One might anticipate that better penetration could substantially improve the overall mixing efficiency, as observed. To summarize, large injection angles are necessary for the required fuel-jet penetration in the aft region of the combustor at this Mach number and equivalence ratio.

The difference in behavior discussed above was captured in the two-way interaction between injector angle and location. Yet this two-way interaction varies with freestream Mach number (M_o). To appreciate this phenomenon, consider the shape of the response surface at ($\phi_{inj} = 1.4, M_o = 12$) which is shown in Figure 15. Notice that there was very little twist in the surface; increasing injector angle improved mixing performance for all injector locations. This is due, in part, to the fact that the combustor inflow condition was substantially more difficult to penetrate with the hydrogen fuel jets at all angles. The high-Mach results tend to share the same characteristic of an oxygen-rich core flow along the flowpath centerline. Another substantial challenge at the high-Mach number limit was alluded to above: the length available for complete mixing is approximately 70% shorter than the low-Mach condition. The statistical description of the above circumstances can be summarized by saying that the variables ($\alpha_{inj}, X_{inj}, M_o$) are involved in a three-way interaction. The interaction can be appreciated in a visual way in Figure 16 by noting the change in twist for the three surfaces shown.

Surrogate-Based Optimization

The GTx configuration has been designed for an accelerator mission. The scramjet operates in a continuous fashion from initiation around Mach 6, to the conclusion about Mach 12. Any performance optimization must take this variable operating condition into account. The great advantage of response surface methods lies in the ability to explore many different optimization schemes with a surrogate-based

approach. Once the regression has been developed and verified, the polynomial representation of performance can be used as a surrogate for the complex and time-consuming CFD simulations. For our purposes, integration of the mixing performance across the scramjet flight condition can be calculated directly for any combination of the design factors. Since we know that the effect of fuel equivalence ratio has a net positive effect on mixing performance, we shall explore the results associated with the maximum value ($\phi_{inj} = 1.4$).

The goal of the optimization is to discover which injector geometry (α_{inj} , x_{inj}) yields the highest net mixing performance across the Mach number range of interest. This geometry must maximize the following condition

$$\int_{6.5}^{12} \eta_{mix}(\alpha_{inj}, x_{inj}, M_0, \phi_{inj} = 1.4) dM_0$$

for all injector geometry combinations (α_{inj} , x_{inj}). Figure 17 shows the graphical image of this condition, and the maximum value (75°, -107.5 in.) is shown with a black dot. Now the mixing performance of this optimal injector geometry can be compared to our stated target performance, shown in Figure 18. The message from this optimization was clear: no geometric injector configuration within this design space can achieve the mixing goal of 92.5% efficiency. Although the performance at the lower Mach numbers is encouraging, the performance rapidly declines to unacceptable levels.

Other optimization strategies can be explored by permitting more than one geometric configuration to be utilized. Two additional attempts have been made, by segmenting the Mach range into multiple segments and repeating the optimization process outlined above. The results, shown in Figure 19, demonstrate that incremental improvements can be made by using one low-angled injector for the first half of the Mach range and a large-angled injector for the high-speed range. The improvement available by changing to three or more separate geometries was negligible. The two-segment optimal design utilized a (15°, -112 in.) injector for the first half of the trajectory, and a (75°, -110 in.) injector second half of the trajectory. The inescapable conclusion here is that we must pursue injector designs beyond this design space to achieve the mixing efficiency required at the high Mach flight conditions.

Finally, little mention has been made of the response surface results concerning the total pressure recovery within the scramjet combustor. At the initiation of the present work, it was my expectation that several different injector configurations would be capable of achieving the desired mixing results. The total pressure recovery was envisioned as a discriminator that would play an important role in definition of the optimal design. Until mixing performance improvements are realized, this data will be of secondary importance to our goal of meeting the target efficiencies.

Conclusions

Statistical Design of Experiments has provided a framework for conducting an efficient and thorough study of the GTx scramjet fuel mixing process. Initial dominant effects were revealed with a five-factor screening design. A detailed four-factor central composite design was used to explore the performance variation across the design space and develop a response surface model capable of resolving a suspected three-way variable interaction. An effective surrogate model was assembled to capture the mixing efficiency results from the twenty-five CFD simulations. This surrogate model provided a cost-effective means of exploring several injector design optimization strategies. The design for maximizing mixing efficiency was observed to be a two-geometry configuration that utilized a (15°, -112 in.) injector for the first half of the scramjet trajectory, and a (75°, -110 in.) injector for the remainder. However, optimization results clearly indicate that the performance capabilities of this injector design fall short of the target during high-Mach scramjet operation. Other design configurations should be included in future analysis of this annular scramjet combustor.

Future Work

To date, the GTX scramjet injector design strategy has utilized the simple approach of flush wall injection. This strategy has several clear advantages, including an unobtrusive design, a long history of both experimental and computational analysis, and an accepted design strategy for layout. Other programs have demonstrated better mixing characteristics by incorporating a mechanism that can enhance streamwise vortical motion and improve the near field mixing of hydrogen fuel jets. The design challenge for a RBCC engine like GTX is to preserve the unobstructed flowpath, and geometric simplicity while generating this vortical flow. Deployable hardware and fixed flow obstructions will be given a low priority due to the inherent complications just discussed. However, the GTX flowpath does present the scramjet designer with a sudden-expansion feature at the combustor inflow plane. The interaction of angled fuel injection from the edge of this sudden expansion is the subject of a current research effort.

Appendix

The response data of Table 2 can readily be turned into a response surface model via regression techniques. The following polynomial expression was derived with the Design Expert software. Note that a natural logarithm transformation of the mixing efficiency data ($\eta_{\text{mix}}^{\text{trans}}$) was performed prior to modeling; the mixing efficiency model is back-transformed via the exponential (EXP) function.

$$\begin{aligned} \left(\eta_{\text{mix}}^{\text{trans}} \right) = & -25.904 + 0.16767 \alpha_{\text{inj}} - 0.50985 x_{\text{inj}} - 0.84107 M_0 \\ & + 3.3006 \phi_{\text{inj}} - 0.0022317 \left(x_{\text{inj}} \right)^2 + 0.040200 \left(M_0 \right)^2 \\ & + 0.0016821 \left(\alpha_{\text{inj}} x_{\text{inj}} \right) - 0.012812 \left(\alpha_{\text{inj}} M_0 \right) \\ & + 0.000044196 \left(x_{\text{inj}} M_0 \right) - 0.19789 \left(M_0 \phi_{\text{inj}} \right) \\ & - 0.00013416 \left(\alpha_{\text{inj}} x_{\text{inj}} M_0 \right) \\ \left(\eta_{\text{mix}} \right) = & 100.0\% \frac{\text{EXP} \left(\eta_{\text{mix}}^{\text{trans}} \right)}{1 + \text{EXP} \left(\eta_{\text{mix}}^{\text{trans}} \right)} \end{aligned}$$

A proper interpretation of this polynomial model of mixing efficiency must include the statistical uncertainty $E_{95\% \text{C.I.}}^{\text{trans}}$. The 95% confidence interval on future prediction of the response is defined below. Note that the uncertainty estimate is based upon Student's t-distribution (t_{student}) and the standard error of regression ($S_{\text{trans}(y \bullet x)}$) for the transformed data.⁶

$$\begin{aligned} E_{95\% \text{C.I.}}^{\text{trans}} & \approx \pm t_{\text{student}} S_{\text{trans}(y \bullet x)} ; t_{\text{student}} = 2.16 ; S_{\text{trans}(y \bullet x)} = 0.17 \\ \eta_{\text{mix}}^{\text{trans}} & \approx 100.0 \frac{\text{EXP} \left(\eta_{\text{mix}}^{\text{trans}} \pm E_{95\% \text{C.I.}}^{\text{trans}} \right)}{1 + \text{EXP} \left(\eta_{\text{mix}}^{\text{trans}} \pm E_{95\% \text{C.I.}}^{\text{trans}} \right)} \end{aligned}$$

Note that a similar set of equations has been developed for the response data corresponding to the total pressure recovery. The pressure recovery data did not require any transformation.

$$\begin{aligned} \left(\frac{P_0}{P_{02}} \right) & = 86.213 - 0.39662 \alpha_{\text{inj}} + 0.0020274 \left(c_{\text{inj}} \right)^2 \\ & - 0.18151 x_{\text{inj}} - 0.0016203 \alpha_{\text{inj}} x_{\text{inj}} - 10.245 M_0 \\ & - 0.0075576 \alpha_{\text{inj}} M_0 + 0.012149 x_{\text{inj}} M_0 \\ & + 0.6508 \left(M_0 \right)^2 - 4.3482 \phi_{\text{inj}} - 1.133 M_0 \phi_{\text{inj}} \\ E_{95\% \text{C.I.}} & \approx \pm t_{\text{student}} S_{(y \bullet x)} ; t_{\text{student}} = 2.1 ; S_{(y \bullet x)} = 0.60 \\ \left(\frac{P_0}{P_{02}} \right)^{95\% \text{C.I.}} & \approx \left(\frac{P_0}{P_{02}} \right) \pm E_{95\% \text{C.I.}} \end{aligned}$$

References

1. Trefny, C.J. "An Airbreathing Launch Vehicle Concept for Single Stage to Orbit," AIAA-99-2730, 35th AIAA/ASME/SAE/ASEE Joint Propulsion Conference and Exhibit, June 20-23, 1999.
2. Steffen, C.J., Jr., "Response Surface Modeling of Combined-Cycle Propulsion Components Using Computational Fluid Dynamics," AIAA-2002-0542, Reno, NV, 2002.
3. Hack, K.J., and Riehl, J.P., "Trajectory Development and Optimization of an RBCC-based Launch Vehicle," AAS 99-347, AAS/AIAA Astrodynamics Specialist Conference, Girdwood, AK, 16-19 August, 1999.
4. Steffen, C.J., Jr., Bond, R.B., and Edwards, J.R., "Three Dimensional CFD Analysis of the GTx Combustor," NASA/TM—2002-211572, prepared for the Joint Subcommittee Meeting sponsored by the Joint Army-Navy-NASA-Air Force, Destin, FL, April 2002.
5. Heiser, W.H., and Pratt, D.T., **Hypersonic Airbreathing Propulsion**. AIAA Education Series, J.S. Przemieniecki, Series Editor-in-Chief, ISBN 1-56347-035-7, 1994, pp. 79-80.
6. **CRC Standard Mathematical Tables**, 28th edition, W.H. Beyer, editor, CRC Press, Boca Raton, FL, 1987.

Table 1. Central composite design:
four parameter design space.

	Min	Mid	Max
α_{inj}	15°	45°	75°
\mathbf{x}_{inj}	Fwd (-115 in.)	Mid (-102.5 in.)	Aft (-90 in.)
M_0	6.5	9.25	12
ϕ_{inj}	1.0	1.2	1.4

Table 2. Central composite design: run matrix and response variables for the 25 cases with an additional confirmation run (#26).

Case#	(α_{in})	(x_{inl})	(M_0)	(ϕ_{inl})	(t_{inl})	(P_{0in} / P_{0ex})
1	15°	-115.0"	6.5	1.4	90.4%	39.20%
2	75°	-115.0"	6.5	1	72.5%	38.71%
3	15°	-90.0"	6.5	1	58.6%	40.70%
4	75°	-90.0"	6.5	1.4	87.1%	29.55%
5	45°	-102.5"	9.25	1.2	85.7%	26.89%
6	15°	-115.0"	12	1	46.4%	38.63%
7	75°	-115.0"	12	1.4	64.7%	25.03%
8	15°	-90.0"	12	1.4	26.0%	30.68%
9	75°	-90.0"	12	1	28.0%	27.86%
10	45°	-102.5"	9.25	1.4	69.7%	24.19%
11	15°	-115.0"	12	1.4	57.6%	31.91%
12	15°	-115.0"	6.5	1	76.0%	44.40%
13	75°	-115.0"	6.5	1.4	79.3%	34.76%
14	75°	-115.0"	12	1	55.0%	32.63%
15	15°	-90.0"	6.5	1.4	74.1%	35.22%
16	75°	-90.0"	12	1.4	36.0%	20.80%
17	45°	-102.5"	6.5	1.2	84.2%	34.32%
18	15°	-102.5"	9.25	1.2	53.8%	32.26%
19	75°	-102.5"	9.25	1.2	62.7%	24.30%
20	45°	-102.5"	12	1.2	43.6%	28.44%
21	75°	-90.0"	6.5	1	69.6%	33.61%
22	45°	-102.5"	9.25	1	57.9%	30.22%
23	15°	-90.0"	12	1	20.8%	37.76%
24	45°	-115.0"	9.25	1.2	60.9%	28.78%
25	45°	-90.0"	9.25	1.2	41.7%	26.09%
26	15°	-115.0"	9.25	1.2	60.2%	33.28%

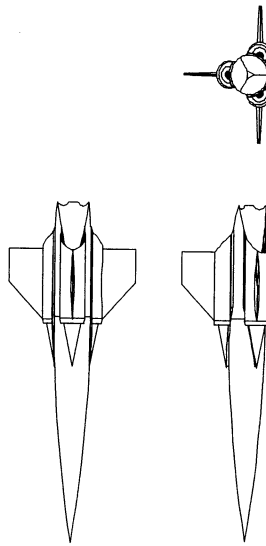


Figure 1. Rocket based combined cycle vehicle geometry: GTX.

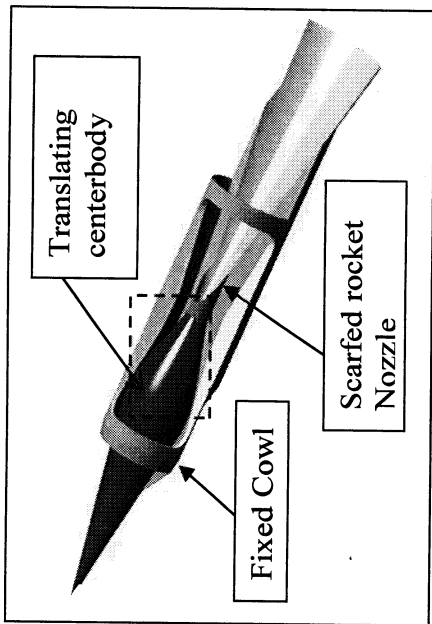


Figure 2. RBCC propulsion system cutaway view.

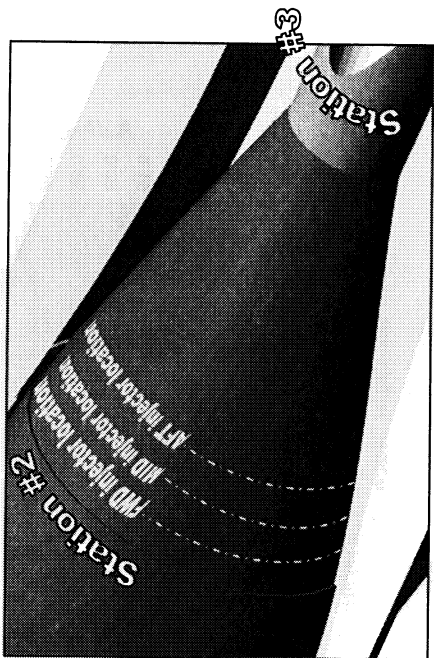


Figure 3. Close-up view of the Scramjet combustor portion of the GTX flowpath.

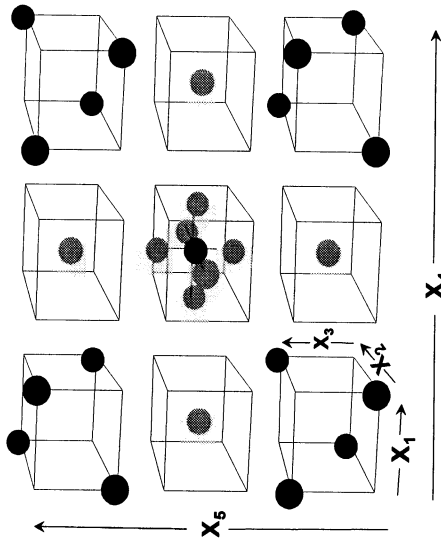


Figure 4. Twenty-seven node fractionated-central-composite design used for screening purposes: this design was for a five parameter, three level analysis.

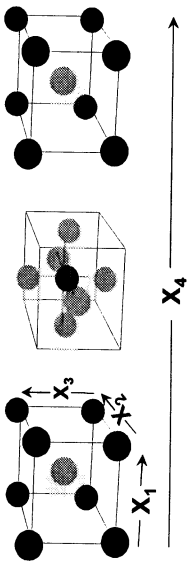


Figure 5. Twenty-five node central-composite design used to build a more accurate response surface model: this design was for a four parameter, three level analysis.

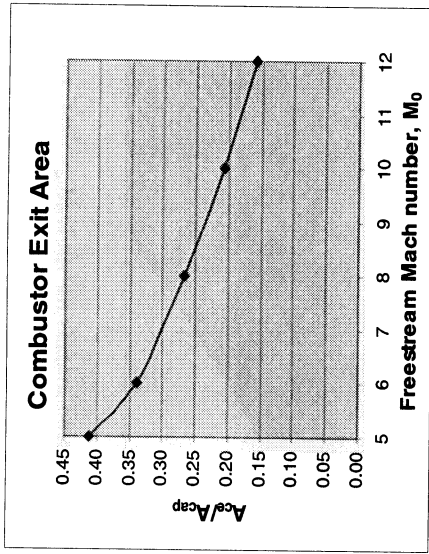


Figure 6. Combustor Exit Area is inversely proportional to the flight Mach number.

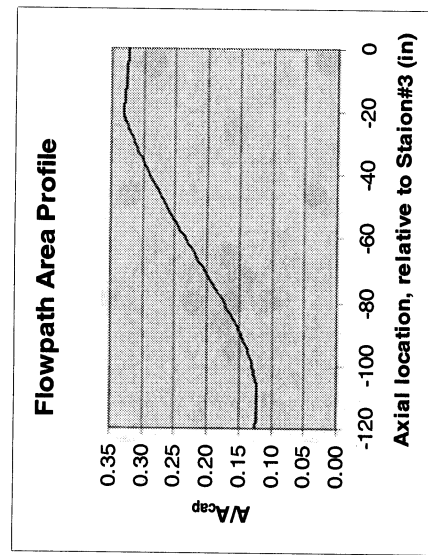


Figure 7. Combustor area profile: note this plot describes the flowpath geometry between stations #2 and #3 depicted above.

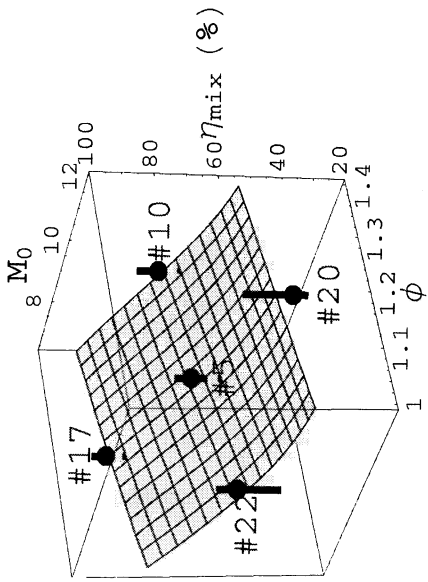


Figure 8. Response surface of mixing efficiency, as a function of flight Mach number (M_0) and fuel equivalence ratio (ϕ).

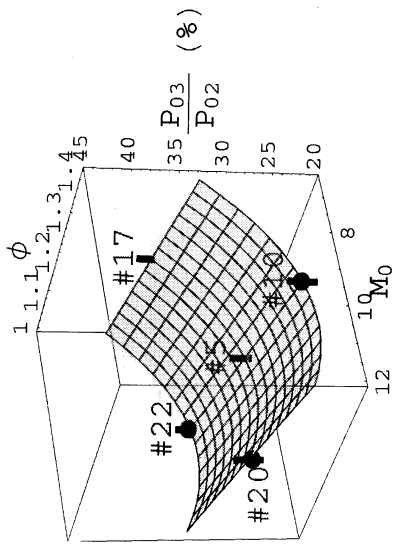


Figure 9. Response surface of total pressure recovery, as a function of flight Mach number (M_0) and fuel equivalence ratio (ϕ).

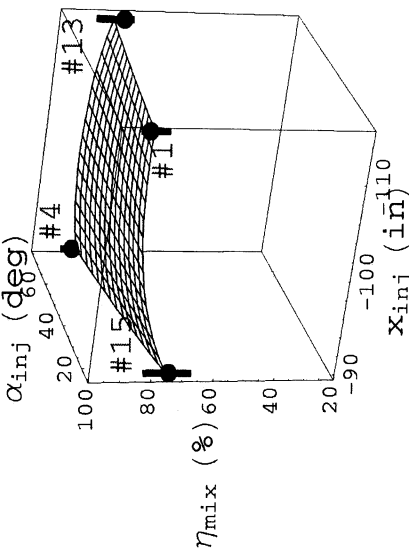


Figure 10. Response surface of mixing efficiency as a function of injector angle (α_{inj}) and location (x_{inj}) for the $M_0 = 6.5, \phi = 1.4$ condition.

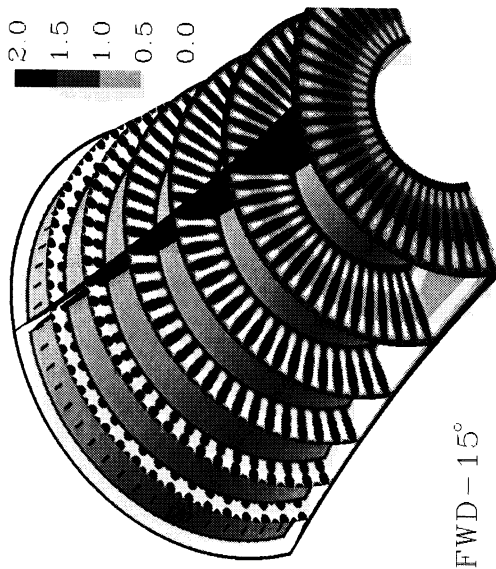


Figure 11. Case #1 (forward-located and low-angled injection):
three-dimensional contours of fuel-equivalence ratio.
Note that the lighter colored regions connote excess oxygen.

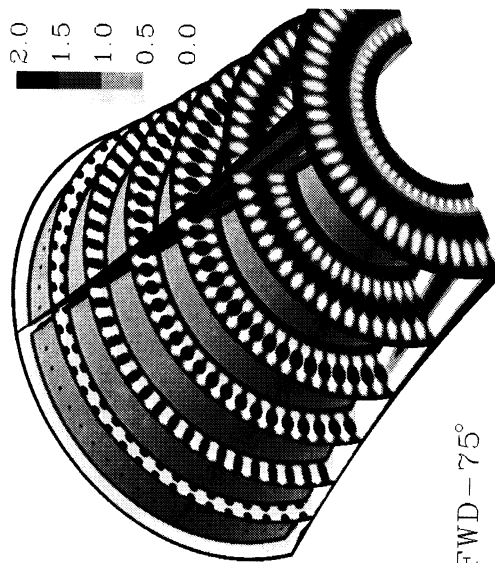


Figure 12. Case #13 (forward-located and high-angled injection):
three-dimensional contours of fuel-equivalence ratio.

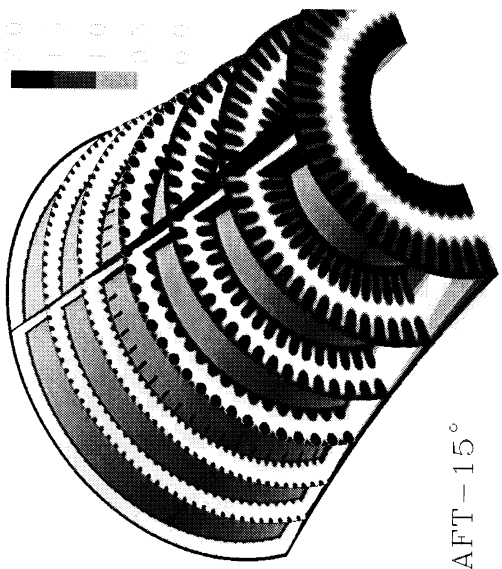


Figure 13. Case #15 (aft-located and low-angled injection):
three-dimensional contours of fuel-equivalence ratio.

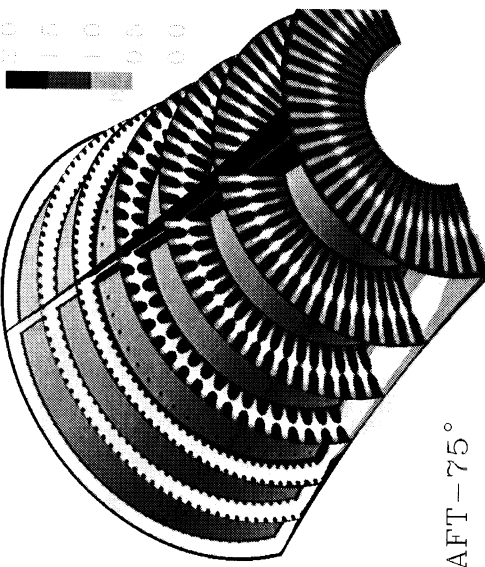


Figure 14. Case #4 (aft-located and high-angled injection):
three-dimensional contours of fuel-equivalence ratio.

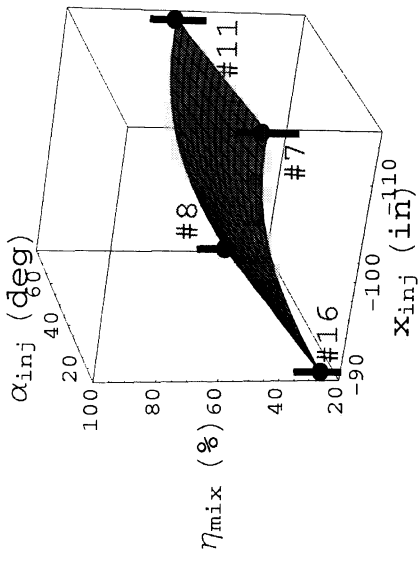


Figure 15. Response surface of mixing efficiency as a function of injector angle (α_{inj}) and location (x_{inj}) for the $M_0 = 12$, $\phi = 1.4$ condition.

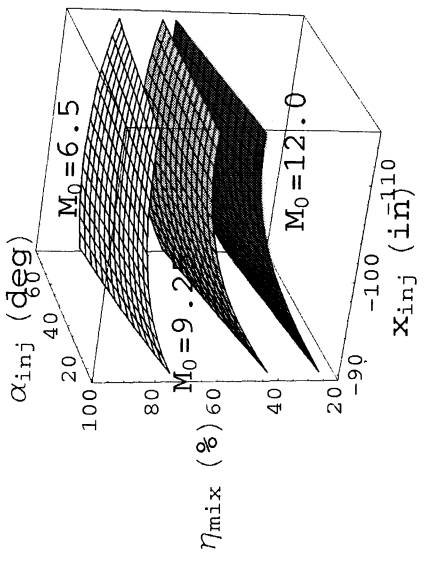


Figure 16. Response surface of mixing efficiency: note the different "surface twist" at each Mach number.

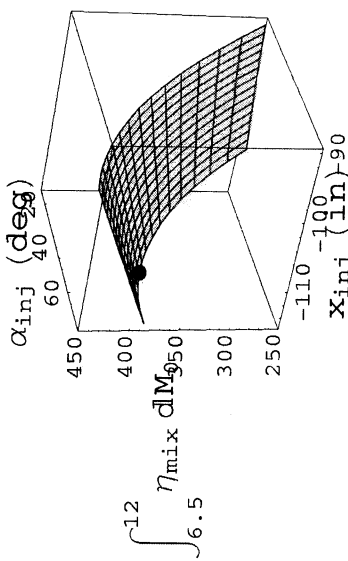


Figure 17. Mixing efficiency, integrated across the flight trajectory of $M_0 = [6.5, 12]$ at $\phi = 1.4$, for all combinations of the injection geometry ($\alpha_{\text{inj}}, x_{\text{inj}}$): note the maximum value shown as a black dot.

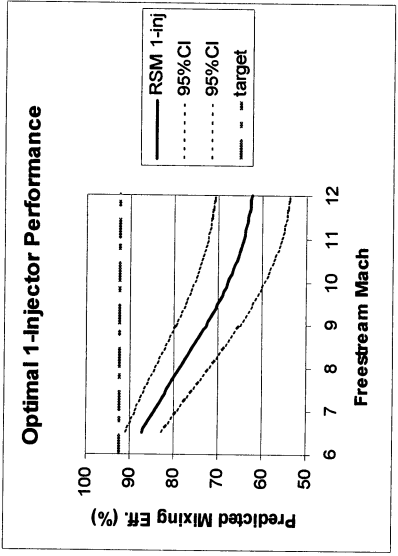


Figure 18. Comparison of the mixing performance of the optimal injector design and the stated target value of 92.5%, across the Mach number range.

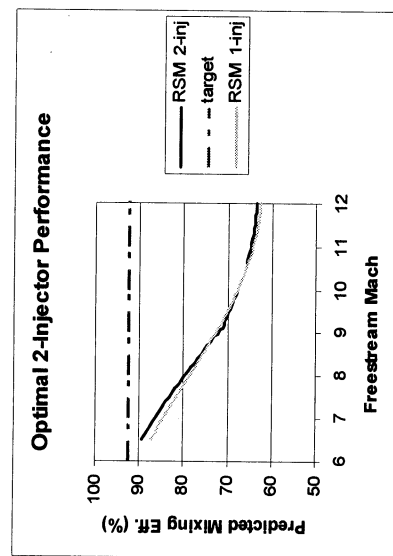


Figure 19. Comparison of two different optimization strategies: the light gray result is the single geometry optimum; the black lines are the two-geometry optimum.

REPORT DOCUMENTATION PAGE

Form Approved

OMB No. 0704-0188

Public reporting burden for this collection of information is estimated to average 1 hour per response, including the time for reviewing instructions, searching existing data sources, gathering and maintaining the data needed, and completing and reviewing the collection of information. Send comments regarding this burden estimate or any other aspect of this collection of information, including suggestions for reducing this burden, to Washington Headquarters Services, Directorate for Information Operations and Reports, 1215 Jefferson Davis Highway, Suite 1204, Arlington, VA 22202-4302, and to the Office of Management and Budget, Paperwork Reduction Project (0704-0188), Washington, DC 20503.

1. AGENCY USE ONLY (Leave blank)	2. REPORT DATE	3. REPORT TYPE AND DATES COVERED	4. TITLE AND SUBTITLE	5. FUNDING NUMBERS
Fuel Injector Design Optimization for an Annular Scramjet Geometry				
6. AUTHOR(S)	WBS-22-708-90-46			
Christopher J. Steffen, Jr.				
7. PERFORMING ORGANIZATION NAME(S) AND ADDRESS(ES)	8. PERFORMING ORGANIZATION REPORT NUMBER			
National Aeronautics and Space Administration John H. Glenn Research Center at Lewis Field Cleveland, Ohio 44135-3191	E-13746			
9. SPONSORING/MONITORING AGENCY NAME(S) AND ADDRESS(ES)	10. SPONSORING/MONITORING AGENCY REPORT NUMBER			
National Aeronautics and Space Administration Washington, DC 20546-0001	NASA TM—2003-212094 AIAA-2003-0651			
11. SUPPLEMENTARY NOTES	Prepared for the 41st Aerospace Sciences Meeting and Exhibit sponsored by the American Institute of Aeronautics and Astronautics, Reno, Nevada, January 6–9, 2003 (invited). Responsible person, Christopher J. Steffen, Jr., organization code 5880, 216-433-8508.			
12a. DISTRIBUTION/AVAILABILITY STATEMENT	12b. DISTRIBUTION CODE			
Unclassified - Unlimited Subject Categories: 15, 34, and 64	Distribution: Nonstandard			
Available electronically at http://gltrs.grc.nasa.gov				
This publication is available from the NASA Center for AeroSpace Information, 301-621-0390.				
13. ABSTRACT (Maximum 200 words)	A four-parameter, three-level, central composite experiment design has been used to optimize the configuration of an annular scramjet injector geometry using computational fluid dynamics. The computational fluid dynamic solutions played the role of computer experiments, and response surface methodology was used to capture the simulation results for mixing efficiency and total pressure recovery within the scramjet flowpath. An optimization procedure, based upon the response surface results of mixing efficiency, was used to compare the optimal design configuration against the target efficiency value of 92.5 percent. The results of three different optimization procedures are presented and all point to the need to look outside the current design space for different injector geometries that can meet or exceed the stated mixing efficiency target.			
14. SUBJECT TERMS	15. NUMBER OF PAGES			
Supersonic combustion ramjet engines; Experiment design; computational fluid dynamics; Rocket-based combined-cycle engines	21			
16. PRICE CODE				
17. SECURITY CLASSIFICATION OF REPORT	18. SECURITY CLASSIFICATION OF THIS PAGE	19. SECURITY CLASSIFICATION OF ABSTRACT	20. LIMITATION OF ABSTRACT	Standard Form 298 (Rev. 2-89) Prescribed by ANSI Std. Z39-18 298-102
Unclassified	Unclassified	Unclassified	Unclassified	NSN 7540-01-280-5500